Development of a mechanistic model of leaf surface gas exchange coupling mass and energy balances for life-support systems applications

Lucie Poulet, Claude-Gilles Dussap, Jean-Pierre Fontaine

Version of Record: https://www.sciencedirect.com/science/article/pii/S0094576520301764
Manuscript_c12e6ce5fa3d1010f79e93f849888deb

Development of a mechanistic model of leaf surface gas exchange coupling mass and energy balances for life-support systems applications

Lucie Poulet[a,b], Claude-Gilles Dussap[a], Jean-Pierre Fontaine[a]

[a] *Université Clermont Auvergne, CNRS, SIGMA Clermont, Institut Pascal, Clermont Ferrand, France*
[b] *Now affiliated at: NASA Kennedy Space Center, Florida, USA*

Abstract

Growing plants in space during long-duration missions will be crucial to ensure functions such as food production, air revitalization, and water purification, and requires an in-depth understanding of plant growth and development processes in reduced gravity. In particular, gas exchange at the leaf surface is considerably reduced because of lack or reduction of buoyancy-driven convection, which can translate into reduced biomass production in the long run. To quantify this impaired gas exchange and biomass production, this study formulates a mechanistic model of these variables in low gravity following a chemical engineering approach. The emphasis here is set on short-term physical response of gas exchange at the leaf surface to gravity and airspeed. A mass balance with stoichiometric limitations enables the computation of mass exchange fluxes, and an energy balance relates them to heat transfer fluxes. Leaf surface temperature and biomass production in the form of dry mass and free water mass are then subsequently computed. The validation of this model on sets of independent data from published parabolic flight experiments is presented and a sensitivity study to different parameters highlights the existence of threshold values for gravity, ventilation, light, and stomatal conductance, which dictate the magnitude of changes in leaf surface temperature and photosynthesis rate. These results show that a mechanistic modeling approach coupled to a dedicated experimental approach are key to identify adequate growth conditions for plants

in reduced gravity environments.

Keywords: Mechanistic model, Gas exchange, Convection, Reduced gravity, Life-Support System, Plants

---

1. Introduction

Integrated within a bioregenerative life-support systems (LSS), plants ensure three crucial and fundamental interdependent functions for human sustainability and survivability: air revitalization, water recycling, and food production [1–7]. To develop robust and reliable LSS and achieve accurate predictive control systems, plants' behavior and development in non-standard environments (e.g. space conditions with low gravity and high radiation levels) must be thoroughly understood and anticipated to deliver the appropriate quantities and quality of substances for human survival [8, 9]. Therefore, the approach followed by the MELiSSA (Micro Ecological Life-Support Alternative) project is to develop mechanistic and knowledge-based models of the processes involved in the LSS before implementing predictive models [10]. Mechanistic models enable a multi-layer and in depth understanding of processes at stake, dividing the analysis into elemental mechanisms at each scale, later integrated back to whole-system variables, while empirical models typically stay at one scale of study, aiming at having a good data fit [11]. This multi-scale approach enables the study of more phenomena at more than just the macroscopic level, and gives more possibilities to improve and manipulate it. However, the large number of hypotheses made at each level can lead to a poorer fit of the model results, relative to empirical models, to experimentally determined data [11].

Typical agronomy models are intended for agricultural decision support, e.g. predicting a certain crop's yield under certain environmental conditions [12–14]; they are excellent predictive tools but do not provide a better understanding of plant growth mechanisms and are not adapted for plants grown in controlled environments [15]. The energy cascade models were specifically developed for controlled-environment agriculture applications in the 1990s, to predict transpiration and biomass production for a large range of environmental parameters on many different candidate species, in particular to help engineers design LSS [15, 16], but they still very much rely on empirical equations. Current

process-based and mechanistic models of gas exchange and heat balance at the leaf surface are designed for crops growing in 1g and do not include a mechanistic definition of the boundary layer thickness based on the limiting heat and mass transfer kinetics [17, 18]. These models typically focus on one aspect of the plant (eg. stomatal conductance, heat balance, photosynthesis) but do not link them together. Another main difference is that models needed for LSS will eventually be used for predicting carbon assimilation, transpiration, and biomass production from a wide range of environmental parameters, while existing process-based models often use these parameters to deduce other aspects such as stomatal conductance, or drought response.

When studying plant growth in confined environments with a mechanistic approach, different scales of study are established, in space and time. First of all, scales linked to the type of processes involved: the morphological scale encompassing the whole plant architecture and structure; the organ scale encompassing physical phenomena; and the cell scale encompassing the biochemical phenomena. Hézard et al. [8] used this approach to develop a plant growth model in the form of a holistic mass balance in 1g, based on Farquhar et al. [19] photosynthesis model, using the single round leaf approximation, and validated and calibrated on data from lettuce grown in controlled-environment chambers [8]. When looking at the physical phenomena, the organ scale can be divided into leaf, roots, and stem (and fruit as needed). The gas exchange phenomena itself can be studied for three distinct spatial scales, at the leaf level, at the whole plant level, or at the canopy level; and three distinct time scales, a short-term physical response linked to the dynamical behavior (fluid dynamics surrounding the leaf), a mid-term biological response linked to the steady-state behavior (stomatal response), and a long-term growth response linked to biomass production.

Buoyancy-driven convection is reduced in low gravity environments, leading to thicker boundary layers around the leaves, which reduce gas exchange at

the leaf surface. This phenomenon has been demonstrated in Earth-orbit and in parabolic flights [20] and can be mitigated by the addition of forced convection [21]. The Grashof dimensionless number (Gr) is the ratio between buoyancy and viscous forces and is proportional to gravity. For a vertical surface of length L with a surface temperature T_S in a bulk air of temperature T_b, it is expressed as follows:

$$Gr = \frac{g\,\beta\,\rho^2\,(T_S - T_b)\,L^3}{\mu^2} \tag{1}$$

g is the gravitational acceleration,β is the coefficient of thermal expansion, ρ is the air density, and μ is the air dynamic viscosity.

Hence, in a given growth chamber at standard pressure, the Grashof number will be respectively 0.166 (1/6) on the Moon and 0.38 (1/3) on Mars, of that on Earth. In future planetary greenhouses, the internal pressure is likely to be reduced to decrease structural constraints, which will affect air density and thus the Grashof number [22]: if the pressure inside a lunar greenhouse is 1/3 of Earth atmospheric pressure, the Grashof number will be 1/54 of that on Earth, which translates to almost negligible natural convection forces. Besides, keeping a homogeneous airflow at each location of a space greenhouse will be challenging, leading to areas where convection is significantly reduced. Hence, it is crucial to have a better understanding of gas exchange phenomena at the leaf surface and how they are linked to convection, in order to predict plant growth in space.

In this study, a chemical engineering approach was used to develop the gas exchange model, based on coupled mass and energy balances, including stoichiometric and kinetics limitations. This model focuses on a short-term dynamic physical response of gas exchange phenomena at the leaf surface. The first step consisted in expanding the initial plant growth model developed by Hézard et al. (a plant growth model based on a mass balance in 1g) to include gravity as an entry parameter. This led to refining the definition of the limiting heat and

mass transfer kinetics via a boundary layer thickness characterization at the leaf surface, coupling mass and energy balances. As a result, a new variable appeared in the system: the leaf surface temperature, linked to the transfer rates.

This study explores the necessary adjustments to model gas exchange at the leaf surface in reduced gravity environments and proposes a new model linking biomass production, leaf surface temperature, and gas exchange. The model is validated on independent sets of data from parabolic flights. The sensitivities to different parameters are studied.

2. Model Presentation

The mechanistic model is based on coupled heat and mass transfers between a solid surface (the leaf surface) and a gas phase with water evaporation in transient regime. In this respect, the guiding equations are issued from a chemical engineering approach. We focused on a dynamic, short-term physical response of the gas exchange at the leaf surface (which differs from a biological or a growth response). For the purposes of the present study we limit the description to the photosynthetic behaviour of the leaf during illuminated periods, neglecting respiration, knowing that other descriptions would have to be developed for other organs and also for dark periods. The leaf being considered as a solid horizontal plate, this results in the assumption that transpiration occurs only on one side of the leaf. First, we defined the stoichiometry of the system; then we defined the mass and heat fluxes associated with this stoichiometry; finally, we defined the kinetics of the system [23]. The symbols and notations used for the model description are summarized in Table 1. The subscript X refers to dry biomass and the subscript FX to fresh biomass. The subscript z refers to the compound z.

Table 1: Summary of the symbols and notations used in the model.

Name	**Symbol**	**Unit**
Plant chamber height	H	m
Gravitational acceleration	g	$m\,s^{-2}$
Bulk air temperature	T_{bulk}	K
Bulk air total pressure	P_{bulk}	Pa
CO_2 partial pressure in bulk air	$p_{bulk}^{CO_2}$	Pa
H_2O partial pressure in bulk air	$p_{bulk}^{H_2O}$	Pa
Bulk air relative humidity	RH	-
Bulk air CO_2 mole fraction	$x_{bulk}^{CO_2}$	ppm
Air density	ρ	$kg\,m^{-3}$

Name	**Symbol**	**Unit**
Air kinematic viscosity	ν	$m^2\,s^{-1}$
Molar air specific heat capacity at constant pressure	C_p	$J\,mol^{-1}\,K^{-1}$
Bulk air velocity	V_{bulk}	$m\,s^{-1}$
Free convection velocity	V_{free}	$m\,s^{-1}$
Forced convection velocity	V_{forced}	$m\,s^{-1}$
Boundary layer thickness	δ	m
Shear stress at the interface between the fluid and the solid surface	τ	Pa
Friction factor	f	-
Reynolds number	Re	-
Transfer coefficient for z	k_z	$m\,s^{-1}$
Diffusion coefficient to z	D_z	$m^2\,s^{-1}$
Leaf surface temperature	T_{leaf}	K
Leaf area	LA	m^2
Specific leaf area	k_1	$m^2\,g^{-1}$
Leaf characteristic length	L	m
Leaf conductance for z	G^z	$mol\,m^{-2}\,s^{-1}$
Boundary layer conductance to z	g^z_{BL}	$mol\,m^{-2}\,s^{-1}$
Stomatal conductance for z	g^z_s	$mol\,m^{-2}\,s^{-1}$
Leaf absorbance	α_{leaf}	-
Temperature in the boundary layer	T_{BL}	K
Stoichiometric yield for z	$Y_{z,X}$	$g_z\,g_X^{-1}$
Molar mass of the carbohydrate equivalent	M_X	$g\,mol_X^{-1}$
Molar mass of the water	M_{H_2O}	$g\,mol_X^{-1}$
Maximum quantum yield	$Y_{C_{photon}}$	$mol_C\,mol_{photon}^{-1}$
Dry mass ratio	ω_X	$g_X\,g_{FX}^{-1}$
Dry mass	m_X	g

Name	**Symbol**	**Unit**
Fresh mass	m_{FX}	g
Water mass in the leaf	m_{H_2O}	g
Water transpiration to water absorption ratio	$\omega_{transpi/abs}$	$-$
CO_2 partial pressure at the leaf surface	$p_{leaf}^{CO_2}$	Pa
H_2O partial pressure at the leaf surface	$p_{leaf}^{H_2O}$	Pa
Water vapor saturating pressure at T_{bulk}	$P^0(T_{bulk})$	Pa
CO_2 partial pressure at the leaf surface	$[CO_2]_{leaf}$	$mol\,m^{-3}$
Partial pressure gradient between the leaf surface and the bulk air for z	Δp^z	Pa
Incident light flux	I_0	$\mu mol\,m^{-2}\,s^{-1}$
Maximum mass exchange fluxes fo z	ϕ_z	$mol\,m^{-2}\,s^{-1}$
Maximum light absorption rate	I^{max}	$mol\,s^{-1}$
Maximum CO_2 uptake rate	$U_{CO_2}^{Max_i}$	$mol\,s^{-1}$
Water transpiration rate	φ_{H_2O}	$mol\,s^{-1}$
Molar water specific heat capacity at constant pressure and 298.15 K	$C_{p_{H_2O}}$	$J\,mol^{-1}\,K^{-1}$
Shortwave energy from incident light	$E^{photons}$	W
Net longwave energy	E^{ray}	W
Convection energy	E^{conv}	W
Transpiration energy	$E^{transpi}$	W
Avogadro number	N_A	mol^{-1}
Planck constant	h	$J\,s$
Light velocity	c	$m\,s^{-1}$
Percentage of the wavelength λ_i	γ_i	$-$
Leaf and surroundings emissivity	ϵ	$-$
Stefan-Boltzmann constant	σ	$W\,m^{-2}\,K^{-4}$
Ideal gas constant	R	$J\,mol^{-1}\,K^{-1}$
Water latent heat of vaporization	λ_{mol}	$J\,mol^{-1}$

2.1. Single-leaf approach

As a first approach, the choice was made to model the plant as a circular single leaf, with a leaf area proportionally increasing with dry biomass production [8]. The single-leaf approach is justified by the fact that upper leaves contribute to most of the gas exchange in a plant, since they are directly under solar radiation and absorb most of it [24].

In an actual plant, an effect to be considered is the mutual aerodynamic interference between leaves, which is not considered in the present model. This is characterized with a shelter factor, translating the decreased exposure of the leaf within a canopy to the free stream air velocity, leading to a decrease in heat and mass transfers [25–27]. The roughness of the leaves also impacts the transfer; a high roughness is associated with a better transfer because it contributes to the boundary layer separation from the leaf surface [25] and leads to turbulent transfer.

2.2. Stoichiometry: dry and fresh mass synthesis

The stoichiometric description only focuses on the photosynthetic metabolism of the leaf, i.e. the absorption of CO_2 and the production of glucose units. We considered that the biomass composition is a polymer of glucose, i.e.: $CH_{1.667}O_{0.833}$. As a first approximation, the basic equation relevant for leaf metabolism is as follows [28]:

$$CO_2 + 0.833\, H_2O \rightarrow CH_{1.667}O_{0.833} + O_2 \tag{2}$$

From equation 2, we deduce a molar ratio of 1 at the leaf level between CO_2 uptake, O_2 production and C-molar production of dry mass, which is in accordance with the results obtained by Hézard [8] based on experiments on lettuce growth in controlled environment.

From equation 2, the molar mass of the carbohydrate equivalent is $M_X = 27\, g\, mol^{-1}$ and the yields $Y_{z,X}$ for water absorption ($z = H_2O$; eq. 3), CO_2 uptake ($z = CO_2$; eq. 4), O_2 production ($z = O_2$; eq. 5), and carbon content ($z = C$; eq. 6) in biomass are:

$$Y_{H_20,\,X} = 0.56\, g_{H_2O}\, g_X^{-1} \tag{3}$$

$$Y_{CO_2,\,X} = 1.63\, g_{CO_2}\, g_X^{-1} \tag{4}$$

$$Y_{O_2,\,X} = 1.19\, g_{O_2}\, g_X^{-1} \tag{5}$$

$$Y_{C,\,X} = 0.444\, g_C\, g_X^{-1} \tag{6}$$

The maximum quantum yield $Y_{C_{photon}}$ is the amount of carbon produced per photon:

$$Y_{C_{photon}} = 0.054\, mol_C\, mol_{photon}^{-1} \tag{7}$$

The dry mass ratio ω_X links fresh mass m_{FX} to dry mass m_X:

$$\omega_X = \frac{m_X}{m_{FX}} \tag{8}$$

$$m_{FX} = m_X + m_{H_2O} \tag{9}$$

m_{H_2O} is the mass of water in the leaf.

2.3. Linking plant morphology to biomass production

The leaf area LA is needed to compute mass transport and heat exchange rates and is proportional to the dry biomass m_X and to the specific leaf area, k_1 in $m^2\, g^{-1}$. k_1 is a species-dependent coefficient and is assessed experimentally to calibrate the model to a given species:

$$LA = \frac{k_1}{\omega_X}\, m_X \tag{10}$$

ω_X is the dry mass ratio introduced in equation 8 and m_X is the dry mass.
The characteristic length of the leaf L is the diameter of the round-shaped leaf:

$$L = 2\sqrt{\frac{LA}{\pi}} \tag{11}$$

2.4. Heat and mass transfers

2.4.1. Introducing gravity as a parameter

The bulk air velocity V_{bulk} is defined as the sum of the free buoyancy-driven convection v_{free} and the forced convection v_{forced}:

$$V_{bulk} = v_{free} + v_{forced} \tag{12}$$

The free convection velocity is expressed as a function of gravity. Applying a global mechanical energy balance between two points with different densities and different heights leads to [29, 30]:

$$\frac{1}{2}\,\rho\, v_{free}^2 = g\,\Delta\rho\, H \tag{13}$$

Then:

$$v_{free} = \sqrt{2\,g\,H\,\frac{\Delta\rho}{\rho}} \tag{14}$$

g is the gravitational acceleration, H is the height of the chamber, $\Delta\rho$ is the density gradient between the bulk air and the leaf surface, ρ is the air density at the leaf surface computed with the partial pressures of each gas and the leaf surface temperature.

2.4.2. Leaf conductance

The leaf conductance for a given compound z refers to its diffusion ability through the leaf, i.e. through the stomata and through the boundary layer between the leaf surface and the bulk gas. The cuticle and mesophyll conductance was neglected here. An electrical analogy is used to compute the total leaf resistance as the sum of the stomatal and boundary layer resistances, which are in series [31, 32]. The leaf conductance G^z for the compound z is the inverse of the leaf resistance:

$$\frac{1}{G^z} = \frac{1}{g_{BL}^z} + \frac{1}{g_s^z} \tag{15}$$

g_{BL}^z and g_s^z are respectively the boundary layer conductance and the stomatal conductance for compound z. Hence:

$$G^z = \frac{g_{BL}^z\, g_s^z}{g_{BL}^z + g_s^z} \tag{16}$$

2.4.3. Boundary layer model

In chemical engineering literature [30, 33], the resistances for momentum, heat and mass transfer between a bulk fluid and a solid surface are represented accounting for a virtual stagnant layer at the interface, the thickness of which characterizes the transfer rates. For a gas phase, the Prandtl and Schmidt

numbers are close to unity and the hydrodynamic, heat and mass boundary layer thicknesses are assumed equal and named δ hereafter. The shear stress at the interface between the fluid and the solid surface, τ_W, is expressed as a function of the boundary layer thickness δ, of the kinematic viscosity ν, of the bulk fluid velocity V_{bulk}, and of the friction factor f:

$$\tau_W = \rho\,\nu\frac{V_{bulk}}{\delta} = \frac{1}{2}f\,\rho\,V_{bulk}^2 \tag{17}$$

ρ is the air density at the leaf surface.

Hence the boundary layer thickness δ is expressed as a function of the friction factor:

$$\delta = \frac{2}{f}\frac{\nu}{V_{bulk}} \tag{18}$$

The friction factor is expressed as a function of the Reynolds number Re and the coefficient ζ, with an empirical correlation:

$$f = \frac{\zeta}{\sqrt{Re}} = \zeta\sqrt{\frac{\nu}{L\,V_{bulk}}} \tag{19}$$

L is the leaf characteristic length.

Finally the boundary layer thickness is given as a function of bulk conditions and fluid conditions:

$$\delta = \frac{2}{\zeta}\sqrt{\frac{\nu\,L}{V_{bulk}}} \tag{20}$$

The values for the coefficient ζ depend on the assumptions supporting the mechanism of the transfer model, ranging from unity for the surface renewal model [34] to 1.33 [35]. In the following sections, we consider the simplest mechanistic interpretation of the surface renewal model: $\zeta = 1$. The transfer coefficients of each compound z in the equivalent stagnant boundary layer k_z are calculated from the thickness of the boundary layer δ and the diffusion coefficient D_z:

$$k_z = \frac{D_z}{\delta} \tag{21}$$

The diffusion coefficients (in $\mathrm{m^2\,s^{-1}}$) are taken from Shewood et al. [33], with P_{bulk} the bulk air total pressure and T_{bulk} the bulk air temperature. D_T is the

heat diffusion coefficient:

$$D_{CO_2} = \frac{0.177}{P_{bulk}\,10^{-1}} \left[\frac{T_{bulk}}{317}\right]^{3/2} \tag{22}$$

$$D_{O_2} = \frac{0.176}{P_{bulk}\,10^{-1}} \left[\frac{T_{bulk}}{298}\right]^{3/2} \tag{23}$$

$$D_{H_2O} = \frac{0.242}{P_{bulk}\,10^{-1}} \left[\frac{T_{bulk}}{293}\right]^{3/2} \tag{24}$$

$$D_T = \frac{0.2207}{P_{bulk}\,10^{-1}} \left[\frac{T_{bulk}}{300}\right]^{1.81} \tag{25}$$

This leads to the following expression for the boundary layer conductance g^z_{BL} in $\mathrm{mol\,m^{-2}\,s^{-1}}$:

$$g^z_{BL} = k_z \frac{P_{bulk}}{R\,T_{BL}} \tag{26}$$

R is the ideal gas constant and T_{BL} is the estimated temperature in the boundary layer taken as the mean temperature between the bulk air and the leaf surface:

$$T_{BL} = \frac{T_{bulk} + T_{leaf}}{2} \tag{27}$$

2.4.4. Stomatal conductance

Experimental measurements show that stomatal conductance not only depends on species and cultivar traits, but also on environmental factors, as well as on the time of the day [36]. Dozens of stomatal conductance models have been developed in the last 50 years [37, 38], from empirical models to mechanistic ones, adapted to water-stressed plants [39], or linking environmental parameters, or photosynthesis to the stomatal conductance [32, 40]. Stomatal conductance modeling is out of the frame of this study, so an average value is taken for stomatal conductance water vapor, that is evaluated for each experimental data set. This modeling choice is justified by the fact that stomatal conductance variations happen over the course of several minutes, while the study here focuses on short (less than a minute) physical responses. The stomatal conductance for CO_2 $g_s^{CO_2}$ is proportional to the stomatal conductance for water vapor

$g_s^{H_2O}$ [31, 41]:

$$g_s^{CO_2} = \frac{D_{CO_2}}{D_{H_2O}} g_s^{H_2O} \tag{28}$$

D_{CO_2} and D_{H_2O} are the diffusion coefficients for CO_2 and water respectively.

2.4.5. Maximum mass fluxes

The approach here follows the one of Hézard et al. [8]. The maximum mass exchange rates for light and CO_2 are computed; they correspond to the mass exchange rates that would be occurring without any metabolic limitations. In a second step, stoichiometric tests determine the limiting rate, be it light-limited or CO_2-limited. Finally, the real mass exchange rates are computed and used to compute the dry biomass production.

The maximum light absorption rate I^{max} in $\mathrm{mol\,s^{-1}}$ for a single leaf is computed with the incident light flux I_0, the leaf absorbance α_{leaf} and the leaf area LA:

$$I^{max} = \alpha_{leaf}\, I_0\, LA \tag{29}$$

In order to determine which rate is limiting, the corresponding maximum CO_2 uptake rate $U_{CO_2}^{Max_1}$ is expressed as a function of the maximum light absorption rate I^{max} and of the maximum quantum yield $Y_{C_{photon}}$ defined in equation 7:

$$U_{CO_2}^{Max_1} = Y_{C_{photon}}\, I^{max} \tag{30}$$

The maximum mass exchange fluxes ϕ_z are driven by the gradients of CO_2 and H_2O partial pressures between the leaf and the bulk air and depend on the leaf conductance for each compound z, G^z:

$$\phi_z = \frac{G^z}{P_{bulk}} \Delta p^z \tag{31}$$

P_{bulk} is the bulk atmospheric pressure and Δp^z is the partial pressure gradient between the leaf surface and the bulk air for the compound z. It is equal to $p_{bulk}^{CO_2} - p_{leaf}^{CO_2}$ for CO_2 and $p_{leaf}^{H_2O} - p_{bulk}^{H_2O}$ for the water vapor, also known as the

vapor pressure deficit (VPD).

Water vapor partial pressure in bulk air $p_{bulk}^{H_2O}$ is computed with the bulk air relative humidity RH and the water vapor saturating pressure at T_{bulk}, $P^0(T_{bulk})$:

$$p_{bulk}^{H_2O} = RH\, P^0(T_{bulk}) \tag{32}$$

$P^0(T_{bulk})$ is computed with Antoine's equation, which gives a semi-empirical relationship between temperature T_{bulk} and vapor pressure of pure components [42, 43]:

$$P^0(T_{bulk}) = 10^5\, 10^{5.4 - \frac{1838.675}{T_{bulk} - 31.737}} \tag{33}$$

H_2O partial pressure at the leaf surface $p_{leaf}^{H_2O}$ is computed assuming saturation at the surface leaf temperature:

$$p_{leaf}^{H_2O} = P^0(T_{leaf}) \tag{34}$$

CO_2 partial pressure in bulk air $p_{bulk}^{CO_2}$ is computed with the bulk air CO_2 mole fraction in ppm $C_b^{CO_2}$ and the bulk air pressure P_{bulk}:

$$p_{bulk}^{CO_2} = C_b^{CO_2}\, P_{bulk} \tag{35}$$

CO_2 partial pressure at the leaf surface $p_{leaf}^{CO_2}$ is computed from the leaf surface CO_2 concentration $[CO_2]_{leaf}$, the leaf surface temperature T_{leaf}, and the ideal gas constant R:

$$p_{leaf}^{CO_2} = [CO_2]_{leaf}\, T_{leaf}\, R \tag{36}$$

The maximum mass exchange rates (in $\mathrm{mol\,s^{-1}}$) for water vapor, φ_{H_2O}, and CO_2, $U_{CO_2}^{Max_2}$, are then computed:

$$\varphi_{H_2O} = \frac{G^{H_2O}}{P_{bulk}} \left(p_{leaf}^{H_2O} - p_{bulk}^{H_2O}\right) LA \tag{37}$$

$$U_{CO_2}^{Max_2} = \frac{G^{CO_2}}{P_{bulk}} \left(p_{bulk}^{CO_2} - p_{leaf}^{CO_2}\right) LA \tag{38}$$

G^{H_2O} and G^{CO_2} are respectively the leaf conductance for water vapor and the leaf conductance for CO_2, P_{bulk} is the bulk air atmospheric pressure, and LA the leaf area.

The two rates $U_{CO_2}^{Max_i}|_{i=1,2}$ are compared and the lowest rate is set to be CO_2 uptake rate. Then, the light absorption rate is computed with respect to this limiting rate and the quantum yield. This way, the stoichiometric limitations are taken into account within the model.

Finally, the water absorption is computed from the water transpiration φ_{H_2O}, using the empirical water transpiration to water absorption ratio $\omega_{transpi/abs}$:

$$U_{H_2O} = \frac{\varphi_{H_2O}}{\omega_{transpi/abs}} \tag{39}$$

The partial pressures for water vapor $p_{leaf}^{H_2O}$ and CO_2 $p_{leaf}^{CO_2}$ at the leaf surface are then:

$$p_{leaf}^{H_2O} = p_{bulk}^{H_2O} + \frac{P_{bulk}}{G^{H_2O}\, LA}\, \varphi_{H_2O} \tag{40}$$

$$p_{leaf}^{CO_2} = p_{bulk}^{CO_2} - \frac{P_{bulk}}{G^{CO_2}\, LA}\, U_{CO_2} \tag{41}$$

2.5. Energy balance

The energy balance in transient state at the leaf surface is [17, 44]:

$$\frac{dT_{leaf}}{dt} = \frac{E_{Acc}}{Cp_{leaf}} = \frac{E_{Acc}}{m_{H_2O}\, Cp_{H_2O}} \tag{42}$$

T_{leaf} is the leaf surface temperature, Cp_{leaf} is the leaf specific heat capacity, Cp_{H_2O} is the liquid water specific heat capacity at constant pressure, heat accumulation into the leaf being mostly due to the water content of the wet mass, and E_{Acc} is defined as follows:

$$E_{Acc} = E_{photons} - E_{ray} - E_{conv} - E_{transpi} \tag{43}$$

$E_{photons}$ is the shortwave energy received from incident radiations of the light

source:

$$E_{photons} = I^{max}\, N_A\, h\, c \sum_{i=\lambda_{min}}^{\lambda_{max}} \frac{\gamma_i}{\lambda_i} \tag{44}$$

I^{max} is the maximum light absorption rate, N_A is the Avogadro number, h the Planck constant, c is the light velocity, and γ_i the percentage of the wavelength λ_i. λ_{min} and λ_{max} are respectively the lowest and highest wavelengths of the light source.

E_{ray} is the net longwave energy lost, when the leaf and the surroundings are assimilated to black bodies:

$$E_{ray} = \varepsilon\, \sigma\, (T_{leaf}^4 - T_{bulk}^4)\, LA \tag{45}$$

ε is the emissivity (equal for the plant and the surroundings), σ the Stefan-Boltzmann constant, T_{leaf} is the leaf surface temperature, T_{bulk} the bulk air temperature, and LA the leaf area.

E_{conv} is the energy lost by convection in the air:

$$E_{conv} = C_p\, k_t\, \frac{P_{bulk}}{R\, T_{bulk}}\, (T_{leaf} - T_{bulk})\, LA \tag{46}$$

C_p is the molar air specific heat capacity at constant pressure, k_t is the heat transfer coefficient defined in equation 21 as a function of the heat diffusion coefficient D_t and the boundary layer thickness δ, P_{bulk} is the atmospheric pressure of the bulk air, T_{leaf} is the leaf surface temperature, T_{bulk} the bulk air temperature, and LA the leaf area.

$E_{transpi}$ is the energy lost by transpiration:

$$E_{transpi} = \lambda_{mol}\, \varphi_{H_2O} \tag{47}$$

λ_{mol} is the water latent heat of vaporization and φ_{H_2O} the water transpiration rate defined in equation 37.

2.6. Biomass production

The model was designed to compute biomass production over time, even if this was not the prime focus of this study. The biomass is split between dry mass m_X and water content m_{H_2O}:

$$\frac{dm_X}{dt} = \frac{M_X}{Y_{CO_2,\,X}}\, U_{CO_2} \tag{48}$$

$$\frac{dm_{H_2O}}{dt} = M_{H_2O}\,(U_{H_2O} - \varphi_{H_2O}) \tag{49}$$

M_X and M_{H_2O} are respectively the carbohydrate equivalent and water molar masses, $Y_{CO_2,\,X}$ is the stoichiometric yield for CO_2, U_{CO_2} is the CO_2 uptake rate, U_{H_2O} is the water uptake rate, and φ_{H_2O} is the water transpiration rate.

2.7. Model summary

To sum up, the three differential equations are (combining equations 10, 29, 31, and 48; equations 33, 39, and 49; and equations 42, 44, 45, 46, and 47):

$$\frac{dm_X}{dt} = \frac{M_X}{Y_{CO_2\,X}}\, U_{CO_2} = \frac{M_X}{Y_{CO_2\,X}}\, Y_{C_{photon}}\, \alpha_{leaf}\, I_0\, \frac{k_1}{\omega_X}\, m_X \tag{50}$$

$$\frac{dm_w}{dt} = M_{H_2O}\, \frac{1-\omega_{transpi/abs}}{\omega_{transpi/abs}}\, f(T_{leaf}) \tag{51}$$

with $\varphi_{H_2O} = f(T_{leaf})$ since $p_{leaf}^{H_2O}$ is computed with Antoine's equation from T_{leaf}.

$$\frac{dT_{leaf}}{dt} = \frac{E_{Acc}}{m_{H_2O}\, Cp_{H_2O}} = \frac{f_1(m_X) - f_2(T_{leaf}^4) - f_3(T_{leaf}) - f_4(T_{leaf})}{m_{H_2O}\, Cp_{H_2O}} \tag{52}$$

with f_1, f_2, f_3, and f_4 functions replacing the whole expressions of $E_{photons}$, E_{ray}, E_{conv}, and $E_{transpi}$ given in equations 44, 45, 46, and 47 respectively. These equations are solved with the ode45 differential equation solver in Matlab.

They involve three variables: the dry biomass m_X and water content m_{H_2O}, which determine the leaf's dimensions, and the leaf surface temperature T_{leaf}. They all need to be initialized at the beginning.

In order to solve these equations, there are seven entry parameters: the stomatal conductance for water vapor $g_s^{H_2O}$, the leaf absorbance α_{leaf}, the acceleration of gravity g, the forced convection velocity v_{forced}, the specific leaf area k_1, the dry mass ratio ω_X, and the transpiration ratio $\omega_{transpi/abs}$.

The rest are environmental parameters: the bulk air temperature T_{bulk}, pressure P_{bulk}, relative humidity RH, and CO_2 content $C_b^{CO_2}$, the light level I_0, the chamber height H; and species-specific morphological parameters: the dry mass ratio ω_X and the transpiration ratio $\omega_{transpi/abs}$.

This model works in three steps: first, a mass balance computes the mass exchange rates and partial pressures at the leaf surface, based on stoichiometric limitations; then an energy balance establishes the link between the leaf surface temperature and the mass exchange rates and partial pressures computed in the mass balance; finally, the integration of the differential equations enables the computation of the biomass production and the leaf surface temperature.

3. Results

3.1. Sensitivity study

Among the different entry parameters listed here above, the ones identified as having the greater influence on the final leaf surface temperature are: the stomatal conductance for water vapor $g_s^{H_2O}$, the leaf absorbance α_{leaf}, the acceleration of gravity g, and the forced convection velocity v_{forced}. Additionally, the leaf shape also significantly influences the final leaf surface temperature. The sensitivity study here focuses on the influence of these parameters on the final leaf surface temperature. Table 2 summarizes the parameters used for the simulations in this study and Table 3 the values of the physical constants. Please note that what is referred to as "0g" throughout this and the following section corresponds in fact to 0.01 x 9.807 m.s^{-2} = 0.01g.

Table 2: Environmental parameters and initialization values for the sensitivity analysis.

Name	**Symbol**	**Value**	**Unit**
Plant chamber height	H	0.3	m
Bulk air temperature	T_{bulk}	293.15	K
Bulk air total pressure	P_{bulk}	101300	Pa
Bulk air relative humidity	RH	0.5	-
Bulk air CO_2 mole fraction	$x_{bulk}^{CO_2}$	700	ppm
Dry mass ratio	ω_X	0.09	$g_X\, g_{FX}^{-1}$
Water transpiration to water absorption ratio	$\omega_{transpi/abs}$	0.9	–
Specific leaf area	k_1	0.0044	$m^2\, g^{-1}$
Incident light flux	I_0	400	$\mu mol\, m^{-2}\, s^{-1}$
Initial fresh mass	m_{FX}	0.3	g
Initial leaf surface temperature	T_{leaf}	295.15	K

Table 3: Physical constants.

Name	**Symbol**	**Value**	**Unit**
Avogadro number	N_A	$6.02\,10^{23}$	mol^{-1}
Planck constant	h	$6.63\,10^{-34}$	$J\,s$
Light velocity	c	$3\,10^{8}$	$m\,s^{-1}$
Leaf and surroundings emissivity	ϵ	0.97	–
Stefan-Boltzmann constant	σ	$5.670\,10^{-8}$	$W\,m^{-2}\,K^{-4}$
Ideal gas constant	R	8.314	$J\,mol^{-1}\,K^{-1}$
Water latent heat of vaporization	λ_{mol}	$4.0788\,10^{4}$	$J\,mol^{-1}$
Molar water specific heat capacity at constant pressure and 298.15 K	$C_{p_{H_2O}}$	75.327	$Jmol^{-1}\,K^{-1}$
Molar air specific heat capacity at constant pressure and 298.15 K	C_p	29.3	$Jmol^{-1}\,K^{-1}$
Air kinematic viscosity	ν	$1.8\,10^{-5}$	$m^2\,s^{-1}$

3.1.1. Stomatal conductance for water vapor and leaf absorbance

The leaf surface temperature is computed with the model for three different forced ventilation v_{forced} values: 0 m s^{-1}, 0.1 m s^{-1}, and 1 m s^{-1}. For each of these airspeed values, three gravity levels are tested: 0g, 1g, and 2g; and for each one, the stomatal conductance for water vapor $g_s^{H_2O}$ varies from 0.1 to 1.0 mol m^{-2} s^{-1} and the leaf absorbance α_{leaf} from 0.5 to 0.9. These results are summarized in Figure 1, Figure 2, and Figure 3.

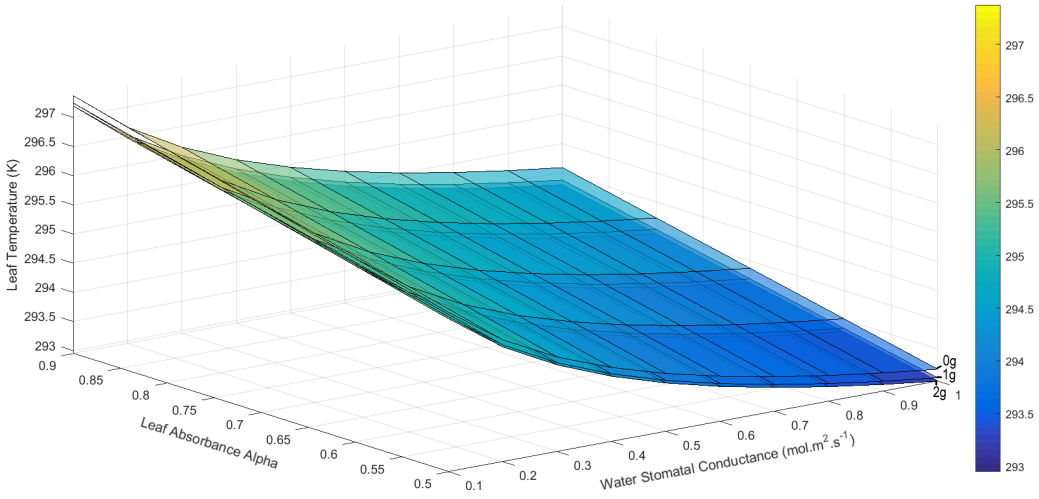

Figure 1: Leaf surface temperature after 20 seconds with a ventilation of 1 m/s

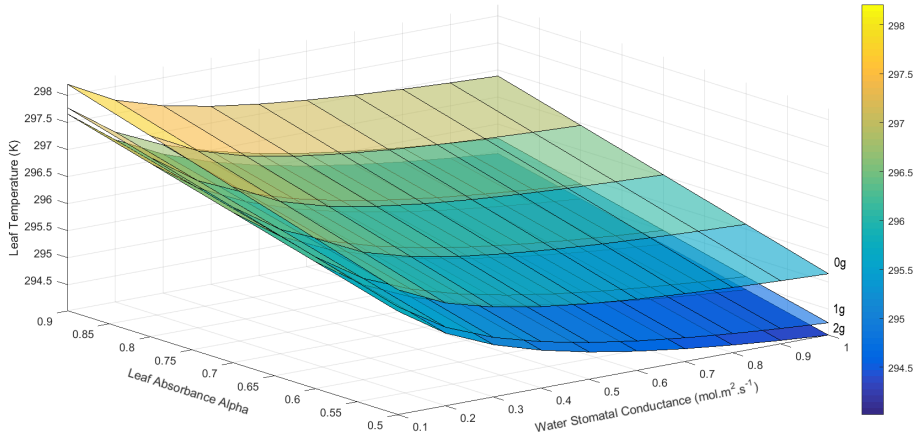

Figure 2: Leaf surface temperature after 20 seconds with a ventilation of 0.1 m/s

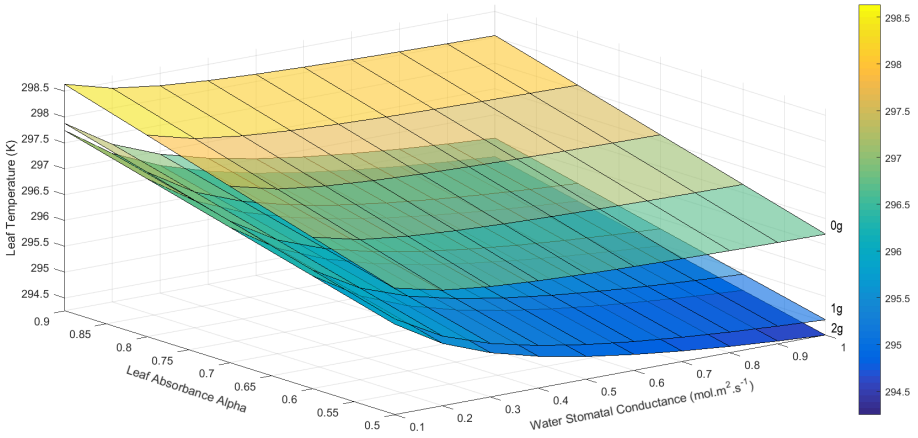

Figure 3: Leaf surface temperature after 20 seconds with a ventilation of 0 m/s

A four-way ANOVA with up to two-way interactions was performed on these final leaf surface temperatures, the four factors being ventilation, gravity, leaf absorbance, and stomatal conductance for water vapor. The ratio of the mean squares, F, and the p-values of the test are given in Table 4.

Table 4: Ratio of the mean squares, F, and p-values of the four-way ANOVA test on all four factors and their two-way interactions.

Factors and Interactions	**F**	**p-value**
Ventilation	13563.07	0.0000
Gravity	5688.41	0.0000
Leaf Absorbance	5208.68	0.0000
Stomatal Conductance for H_2O	2616.68	0.0000
Ventilation*Gravity	1181.57	0.0000
Ventilation*Leaf Absorbance	7.4	0.0000
Ventilation*Stomatal Conductance for H_2O	120.66	0.0000
Gravity*Leaf Absorbance	8.41	0.0000
Gravity*Stomatal Conductance for H_2O	39.33	0.0000
Leaf Absorbance*Stomatal Conductance for H_2O	1.3	0.1207

As expected, the lowest leaf surface temperature increase occurs for cases at 2g in all ventilation settings (Figures 1, 2, 3). With no ventilation at 0g, the leaf surface temperature increases for all values of leaf absorbance (α_{leaf}) and stomatal conductance for H_2O ($g_s^{H_2O}$) (Figure 3). The difference between the three gravity levels decreases with the addition of forced ventilation, even as low as 0.1 m/s: at the lowest leaf absorbance and highest stomatal conductance for water vapor, the leaf surface temperature decreases at 0g at 0.1 m/s (Figure 2). The results of the the four-way ANOVA test reported in Table 4 show that all four factors (ventilation, gravity, leaf absorbance, and stomatal conductance for water vapor) have a significant effect on the final leaf surface temperature (p-values lower than 0.05). It also shows that the effect of ventilation is dependent on the gravity level, on the leaf absorbance, and on the stomatal conductance for water vapor; and that the effect on gravity depends on the leaf absorbance, and on the stomatal conductance for water vapor. However there is no interaction between leaf absorbance and stomatal conductance for water vapor (p-value of

0.1207, greater than 0.05). A one-way ANOVA test on the factor gravity and a multiple pairwise comparison (Tukey's HSD test) shows that the groups 1g and 2g are never significantly different, regardless of the ventilation, leaf absorbance, or stomatal conductance for water vapor (Figure 4), but that they are always significantly different from the 0g group.

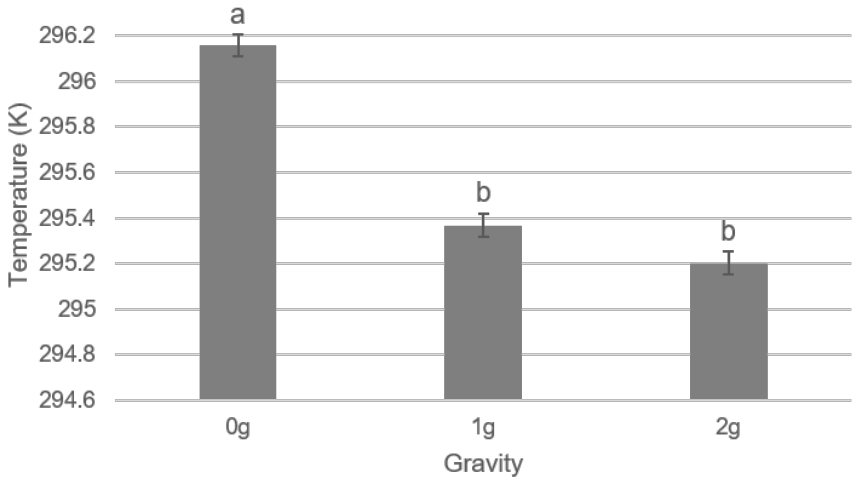

Figure 4: Average leaf surface temperature after 20 seconds, over all values of ventilation, leaf absorbance and stomatal conductance, for three different groups of gravity. The letters indicate the results of the multiple pairwise comparison. The error bars indicate the variability across the different values of ventilation, leaf absorbance and stomatal conductance.

A one-way ANOVA test on the factor ventilation and a multiple pairwise comparison (Tukey's HSD test) reveals that each ventilation group is significantly different from one another and can thus be studied as independent subgroups. At 1 m/s, a one-way ANOVA test on the factor gravity leads to a p-value of 0.5868, indicating that no gravity group is significantly different at that ventilation, so the final leaf surface temperatures are not statistically significantly different between gravity levels, regardless of the values of α_{leaf} and $g_s^{H_2O}$. This is well shown on Figure 1 where the gaps between the three gravity levels are

minimal with a ventilation of 1 m/s. At 0 m/s and 0.1 m/s, a multiple pairwise comparison (Tukey's HSD test) shows that the group 0g is significantly different from the two others (1g and 2g), but that there is no statistically significant difference between 1g and 2g, regardless of the values of α_{leaf} and $g_s^{H_2O}$.
As expected also, the lowest (respectively highest) temperature increases are found with the combination of the highest (respectively lowest) absorbance and lowest (respectively highest) conductance for all ventilation and gravity levels (Figures 1, 2, 3). The leaf surface temperature increase is greater for a higher leaf absorbance α_{leaf} value than for a low stomatal conductance for water vapor $g_s^{H_2O}$ value: at 1 m/s, there is a one-degree gap between the leaf surface temperature at high $g_s^{H_2O}$, high α_{leaf} and the leaf surface temperature at low $g_s^{H_2O}$, low α_{leaf} (Figure 1). For low airspeed at 0g (Figures 2, 3), the influences of stomatal conductance for water vapor are less visible but the slope generated by the influence of leaf absorbance remains the same for the three gravity levels for the three 3 airspeed values, about +1.5 degree regardless of the value of $g_s^{H_2O}$. With no ventilation, leaf surface temperature decreases at 1g for $\alpha_{leaf} = 0.6$ and $g_s^{H_2O} = 0.7..1.0$ and for $\alpha_{leaf} = 0.5$ and $g_s^{H_2O} = 0.4..1.0$; and at 2g for $\alpha_{leaf} = 0.7$ and $g_s^{H_2O} = 0.8..1.0$, for $\alpha_{leaf} = 0.6$ and $g_s^{H_2O} = 0.5..1.0$ and for $\alpha_{leaf} = 0.5$ and $g_s^{H_2O} = 0.3..1.0$.

3.1.2. Leaf shape

As detailed in section 2.1, the leaf in the model is assumed to be circular-shaped. The leaf shape has an effect on its characteristic length, which is a parameter in the boundary layer thickness equation (see equation 18). Here we studied the influence of two different types of leaf shapes with equal surface areas on leaf surface temperature: circular, with the leaf diameter as characteristic length; rectangular, with a width of 2 cm and the characteristic length being the leaf area divided by this width. For these simulations, the leaf absorbance is set to 0.7 and the stomatal conductance for water vapor is set to 0.5; the leaf area is 0.0013 m^2. The results are given in Figure 5.

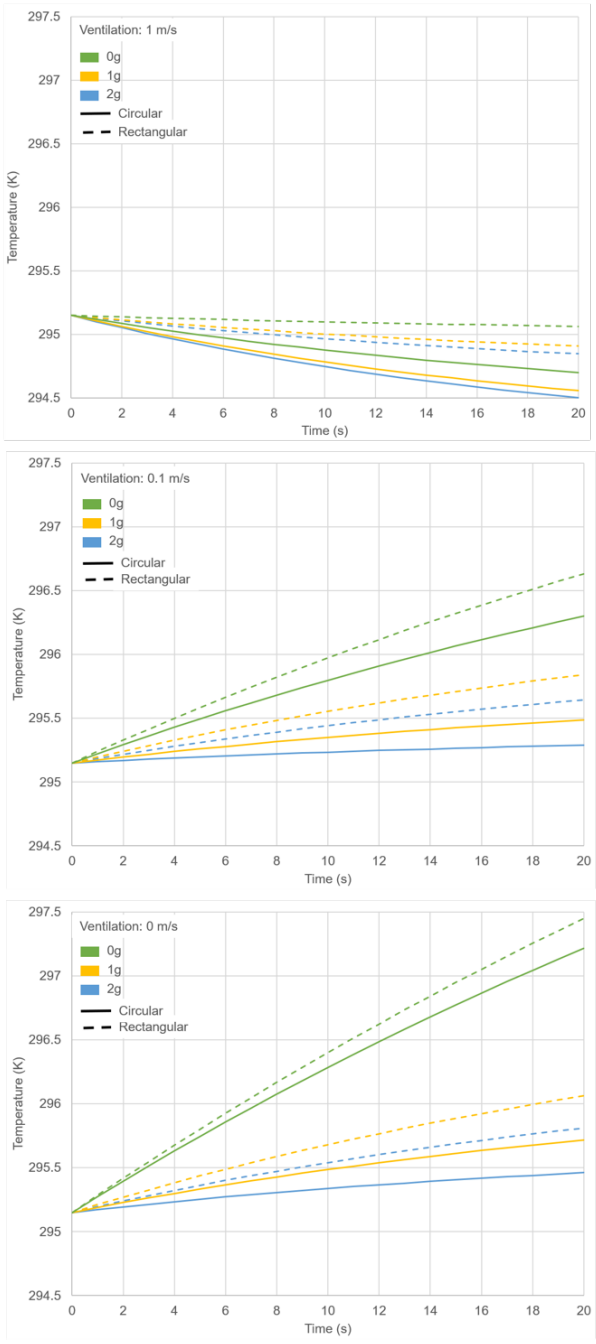

Figure 5: Leaf surface temperature for a circular and a rectangular leaf in three gravity levels. Top: ventilation of 1 m/s; Middle: ventilation of 0.1 m/s; ventilation of 0 m/s. The solid/dotted lines are the circular/rectangular leaf temperatures.

The leaf surface temperature of the circular-shaped leaf is always lower than that of a rectangular-shaped leaf, regardless of the gravity and ventilation levels (Figure 5). This can be explained by the fact that the characteristic length of a rectangle with a width of 2 cm is larger than the diameter of a disk of the same surface; the resulting boundary layer thickness is thus larger and the direct consequence of a larger boundary layer is a higher leaf surface temperature. With no ventilation or 0.1 m/s, the difference in the rise of leaf surface temperature for a circular-shaped leaf and that for a rectangular-shaped leaf is larger at 1g and 2g than at 0g (Figure 5). A three-way ANOVA, with up to two-way interactions, was performed on final leaf surface temperatures, the three factors being: ventilation, gravity, and leaf shape. The ratio of the mean squares, F, and the p-values of the test are given in Table 5.

Table 5: Ratio of the mean squares, F, and p-values of the three-way ANOVA test on all three factors and their two-way interactions.

Factors and Interactions	**red**F	**p-value**
Ventilation	265.31	0.0000
Gravity	105.82	0.0000
Leaf Shape	36.78	0.0000
Ventilation*Gravity	20.31	0.0000
Ventilation*Leaf Shape	0.14	0.8713
Gravity*Leaf Shape	0.11	0.8914

All three factors, gravity, ventilation, and leaf shape have a significant effect on the leaf surface temperature. However the interaction terms between leaf shape and ventilation, and between leaf shape and gravity show a p-value far above 0.05, inferring that for some combinations of leaf shape and ventilation or gravity, there is no significant effect on leaf temperature. For each ventilation group, a two-way ANOVA test and a multiple pairwise comparison (Tukey's HSD test) enable the study of these relationships (Figure 6).

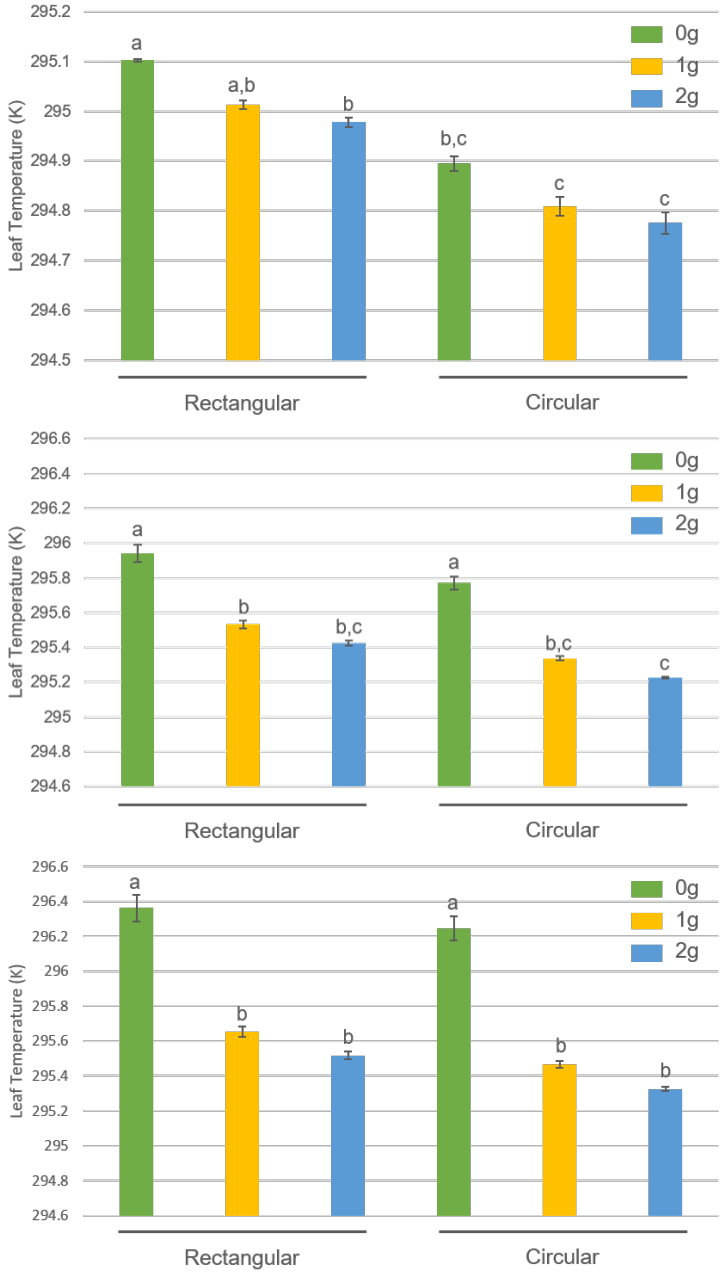

Figure 6: Average leaf surface temperatures over 20 seconds for two different leaf shapes and three gravity levels. Top: ventilation of 1 m/s; Middle: ventilation of 0.1 m/s; ventilation of 0 m/s. The letters indicate the results of the multiple pairwise comparison between all cases across the two factors, leaf shape and gravity level. The error bars indicate the variability over a time span of 20 seconds.

For the low ventilation cases, the leaf surface temperatures for a circular- and rectangular-shaped leaf are not significantly different in any gravity level (but there is a significant difference between leaf temperatures at 0g and the other two levels) (Figure 6). At 1m/s, the leaf surface temperatures of a circular- and rectangular-shaped leaf are significantly different, regardless of the gravity level (Figure 6).

3.2. Model validation using short-term experiments

To validate the robustness of the model, we tried it on data from the literature. Kitaya et al. [20, 45] reported on experiments performed in parabolic flights aiming at measuring the leaf surface temperature of barley and sweet potato leaves in two different ventilation settings (0.2 and 1 m/s), and the photosynthesis rate of a barley leaf in different environmental conditions, for two different light settings (250 and 500 $\mu mol\, m^{-2}\, s^{-1}$). Barley is a rectangular-shaped leaf; sweet potato is a circular-shaped leaf. Their specific leaf area is different from the one used in the sensitivity study. Environmental parameters differed too, since these experiments took place in a plane. The parameters that differ from the sensitivity study are summarized in Table 6 and 7.

Table 6: Environmental parameters and initialization values for the leaf surface temperature experiment.

Name	**Symbol**	**Value**	**Unit**
Bulk air temperature	T_{bulk}	299.15	K
Bulk air total pressure	P_{bulk}	91170	Pa
Bulk air relative humidity	RH	0.15	-
Specific leaf area barley leaf	k_1	0.0061	$m^2\,g^{-1}$
Specific leaf area sweet potato leaf	k_1	0.0057	$m^2\,g^{-1}$
Irradiance at the leaf surface	Irr	260	$W\,m^{-2}$
Conversion factor from $W\,m^{-2}$ to $mol\,m^{-2}\,s^{-1}$ for incandescent lamp	$Conv$	$5\,10^{-6}$	$mol\,J^{-1}$
Incident light flux	I_0	Irr x $Conv$	$\mu mol\,m^{-2}\,s^{-1}$
Initial fresh mass	m_{FX}	0.328	g
Initial leaf surface temperature barley leaf at 0.2 m/s	T_{leaf}	303.25	K
Initial leaf surface temperature barley leaf at 1 m/s	T_{leaf}	298.15	K
Initial leaf surface temperature sweet potato leaf at 0.2 m/s	T_{leaf}	306.35	K
Initial leaf surface temperature sweet potato leaf at 1 m/s	T_{leaf}	301.15	K

Table 7: Environmental parameters and initialization values for the photosynthesis rate experiment.

Bulk air temperature	T_{bulk}	293.15	K
Bulk air total pressure	P_{bulk}	91170	Pa
Bulk air relative humidity	RH	0.65	-
Bulk air CO_2 mole fraction	$x_{bulk}^{CO_2}$	380	ppm
Specific leaf area barley leaf	k_1	0.0061	$m^2\, g^{-1}$
Incident light flux	I_0	500	$\mu mol\, m^{-2}\, s^{-1}$
Initial fresh mass	m_{FX}	0.328	g
Initial leaf surface temperature	T_{leaf}	293.15	K

3.2.1. Temperature trends

Stomatal conductance for water vapor and leaf absorbance were not reported in Kitaya et al. [20], therefore we used best estimates on these parameters, which enabled our model to fit their experimental values. The leaf absorbance was set to $\alpha_{leaf} = 0.9$ for both leaves and the two ventilation settings, which is consistent with values found in the literature [18, 46]. For the barley leaf, values of stomatal conductance for water vapor that enabled a good fit between the model and the experimental values was $g_s^{H_2O} = 0.1675\, mol\, m^{-2}\, s^{-1}$ at 0.2 m/s and $g_s^{H_2O} = 0.442\, mol\, m^{-2}\, s^{-1}$ at 1 m/s. For the sweet potato leaf, values of stomatal conductance for water vapor that enabled a good fit between the model and the experimental values was $g_s^{H_2O} = 0.0602\, mol\, m^{-2}\, s^{-1}$ at 0.2 m/s and $g_s^{H_2O} = 0.166\, mol\, m^{-2}\, s^{-1}$ at 1 m/s. The results of these simulations are presented in Figures 7 and 8 and are compared to the values reported by Kitaya et al. [20].

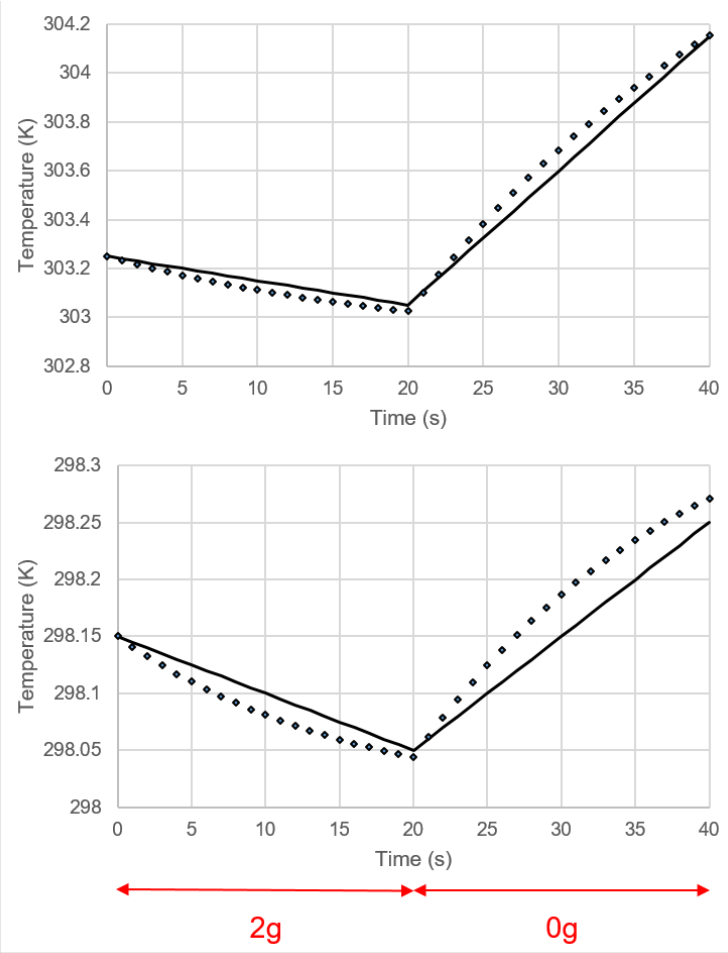

Figure 7: Leaf surface temperature change over the course of 40 seconds for a barley leaf, in a 2g phase followed by a 0g phase. Top: with a forced ventilation of 0.2 m/s; bottom: with a forced ventilation of 1 m/s. Data reported by Kitaya et al. [20] in solid line; simulation results from this model in diamond markers.

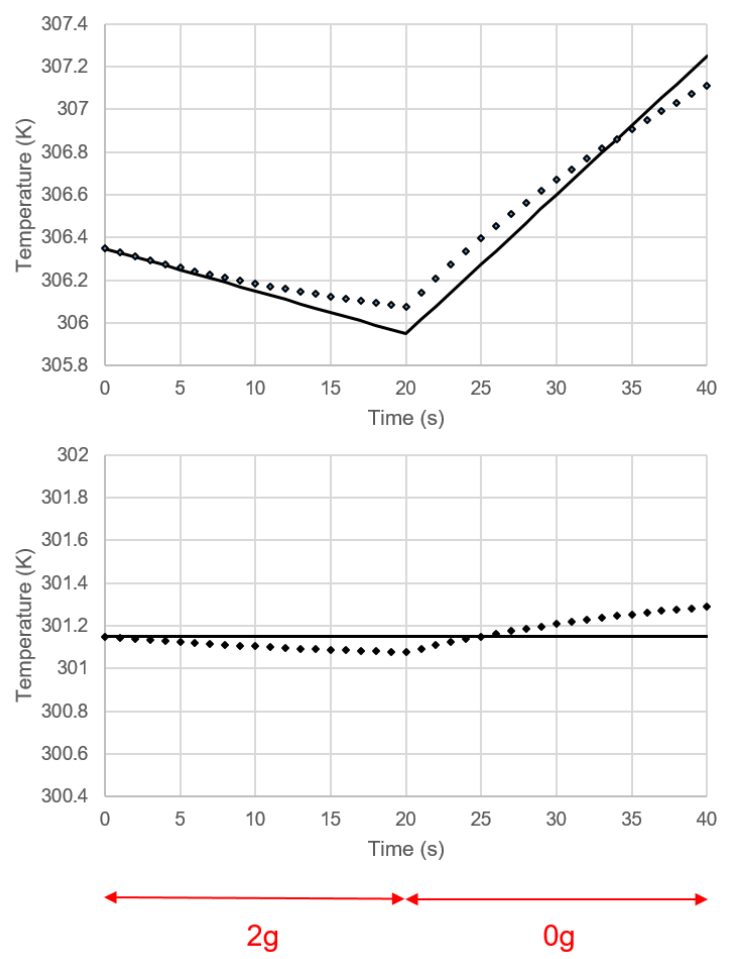

Figure 8: Leaf surface temperature change over the course of 40 seconds for a sweet potato leaf, in a 2g phase followed by a 0g phase. Top: with a forced ventilation of 0.2 m/s; bottom: with a forced ventilation of 1 m/s. Data reported by Kitaya et al. [20] in solid line; simulation results from this model in diamond markers.

The variations of the barley leaf surface temperature are a good fit at 2g and at 0g in terms of trends and magnitudes (Figure 7). For the sweet potato leaf, the fit is not as good, although the magnitude of variations is the same (Figure 8). At low ventilation for both leaves, the leaf surface temperature increase during the 0g phases has a significantly steeper slope than the decrease over the 2g

phase (5.5 fold for the barley leaf at 0.2 m/s, 3.25 for the sweet potato leaf at 0.2 m/s). At 1 m/s, the sweet potato leaf surface temperature has a stable temperature throughout the gravity phases and for the barley leaf, the slope in the 0g phase is 2-fold that of the 2g phase. This is consistent with the results from the sensitivity analysis on the leaf shape: the sweet potato leaf that is circular-shaped has a lower temperature increase and decrease than the barley leaf, which is rectangular-shaped. Results with the highest ventilation (1 m/s) showing little variations in the leaf surface temperature throughout the gravity phases are also consistent with the sensitivity analysis results presented in Figure 1, showing insignificant variations between the gravity levels at 1 m/s. The model presented here has thus enabled us to accurately identify the values of stomatal conductance for water vapor, for two types of leaf shapes in two different ventilation settings, over a short-time dynamic response.

3.2.2. Photosynthesis rate

In Kitaya et al. [45], barley leaf net photosynthesis rate is reported for two different light settings during parabolic flight experiments. The value of stomatal conductance for water vapor that enabled a good fit between the model and the experimental values was $g_s^{H_2O} = 0.018\, mol\, m^{-2}\, s^{-1}$ at 500 $\mu mol\, m^{-2}\, s^{-1}$ and $g_s^{H_2O} = 0.013\, mol\, m^{-2}\, s^{-1}$at 250 $\mu mol\, m^{-2}\, s^{-1}$. Simulation results and experimental data from Kitaya et al. [45] are reported in Figure 9.

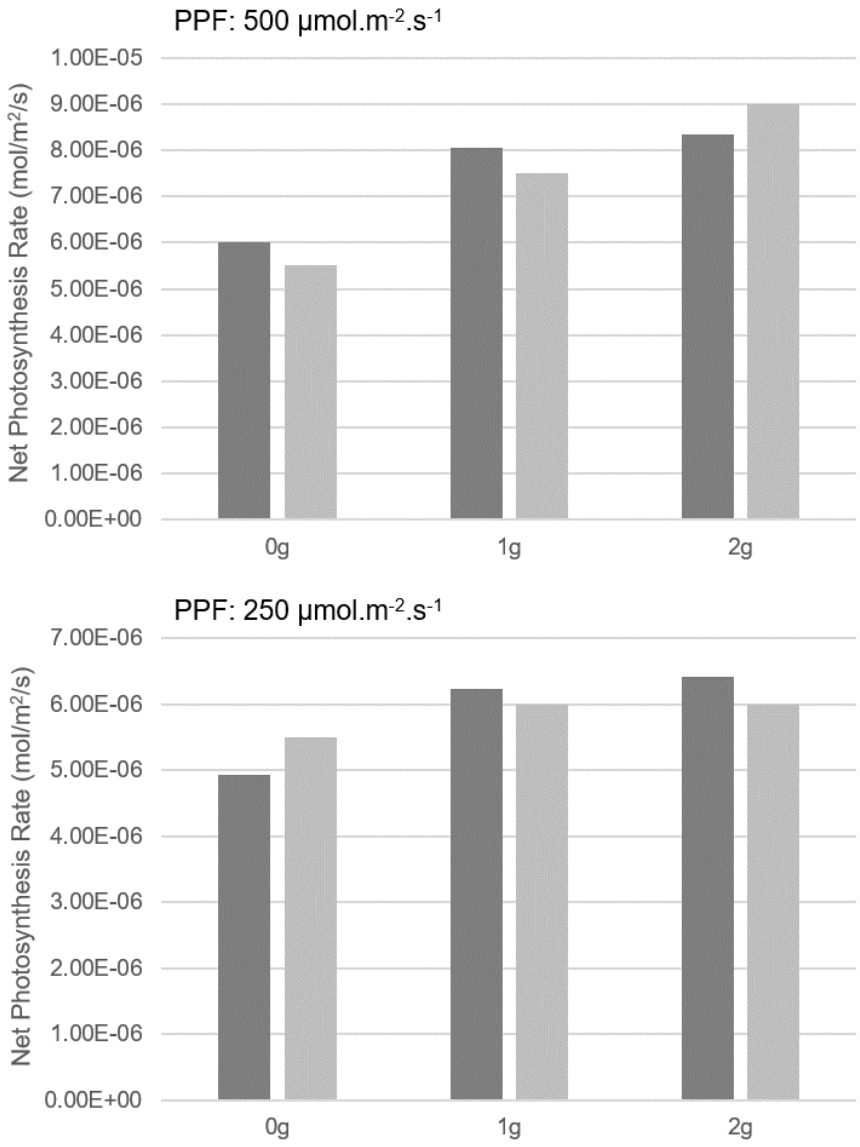

Figure 9: Net photosynthesis rate of a barley leaf in three different gravity settings. Top: 500 $\mu mol\, m^{-2}\, s^{-1}$; bottom: 250 $\mu mol\, m^{-2}\, s^{-1}$. Model results are in dark grey; experimental results reported by Kitaya et al. [45] are in light grey.

At both light levels, the model estimations are within 10% of the experimen-

tal data reported by Kitaya et al. [45]. At 250 $\mu mol\, m^{-2}\, s^{-1}$, they are respectively 90%, 104%, and 107% of the reported values at 0g, 1g, and 2g; at 500 $\mu mol\, m^{-2}\, s^{-1}$, they are respectively 109%, 107%, and 93% of the reported values at 0g, 1g, and 2g. The simulated values show the same trends for both light levels with a difference between the photosynthesis rate at 0g and that at 1g being one order of magnitude greater than that between 1g and 2g. This is also the case for experimental data at 250 $\mu mol\, m^{-2}\, s^{-1}$, but not at 500 $\mu mol\, m^{-2}\, s^{-1}$ (the difference between photosynthesis rates at 0g and 1g, and between that at 1g and 2g is of the same order of magnitude). This shows that the model can accurately predict orders of magnitude for a leaf photosynthesis rate in various gravity levels.

4. Discussion

4.1. Sensitivity to gravity, airspeed, stomatal conductance for water vapor, and light

4.1.1. Gravity

Data reported in Figures 1, 2, and 3 indicate that there is a gravity threshold, above which leaf surface temperatures, and thus gas exchange, are not statistically significantly different (temperatures at 1g and 2g are never statistically different regardless of the ventilation level, but temperatures at 0g and 1g are almost always statistically different). This is especially true for lower ventilation settings. In the same way, there is a ventilation threshold, under which leaf surface temperatures, and gas exchange, are significantly affected by low gravity levels. This is in accordance with the findings of Kitaya et al. [20] in their study of air current velocity effects on sweet potato leaves and a canopy of tomato seedlings in 1g. They advocated a minimum ventilation of 0.2 m/s in the vicinity of the leaves and of 1 m/s above the plant canopy for optimal gas exchange. However, these values should be tailored for different plant species, canopy sizes, and leaf shapes. Finding the lowest ventilation setting for optimal gas exchange is a critical point for large-scale food production because this would prevent energy waste of excessive fan power, as well as lower the risk of mechanical stress induced by high convection around the plants [47, 48].

4.1.2. Airspeed

The values of stomatal conductance for water vapor found for the two parabolic flight experiments reported by Kitaya et al. [20, 45] are larger for higher airspeed. This is not in accordance with the findings of Schymanski et al. [49]. They found that transpiration rate and stomatal conductance for water vapor decreased with increasing wind speeds, when stomatal conductance for water vapor stays under 0.4 $mol\,m^{-2}\,s^{-1}$. Indeed, then, the dominant process to remove heat from incoming shortwave and longwave energy is the sensible heat flux and not the transpiration flux. However, this is true for a constant leaf-air temperature

gradient. In the case of the parabolic flight experiments reported here, the leaf-air temperature gradient was greater at low airspeed (between +4 and +5 K for barley and between +7 and +8 K for sweet potato) than at high airspeed (around -1 K for barley and around +2 K for sweet potato). This means that at low airspeed the sensible heat flux was greater than at high airspeed and that necessarily the latent heat flux was lower at low airspeed, which translates into a smaller stomatal conductance for water vapor. It should be noted that the smallest stomatal conductance for water vapor value (0.0602 $mol\,m^{-2}\,s^{-1}$) was found for the sweet potato leaf at an airspeed 0.2 m/s, which corresponds to the greatest leaf-air temperature gradient (+ 7 to +8 K), while the largest value of stomatal conductance for water vapor (0.442 $mol\,m^{-2}\,s^{-1}$) was found for the barley leaf at an airspeed 1 m/s, which corresponds to the smallest leaf-air temperature gradient (-1 K).

4.1.3. Stomatal conductance for water vapor

At 0g and low airspeed, the effects of stomatal conductance for water vapor on leaf surface temperature are significantly greater for larger values of $g_s^{H_2O}$ (see Figure 3), indicating that, in these conditions, well-watered plants (high $g_s^{H_2O}$) will have a much higher leaf surface temperature, indicating impaired gas exchange, than well-watered plants in higher gravity levels, whereas this difference between gravity levels will be minimal for plants under drought-condition (low $g_s^{H_2O}$). This can be explained by the fact that gas exchange is limited during a drought, because of the lower stomatal conductance for water vapor and thus the effects of other environmental parameters (gravity, ventilation) are of lower magnitude. This analysis not only shows that gravity and ventilation both play a significant role in final leaf surface temperature, but also that plant water status needs to be accounted for. The absence of water stress is one of the main assumptions for plants grown in controlled environments, particularly in bioregenerative life-support systems, so this is an important result for future plant growth in space.

4.1.4. Light

In lower light settings, the reported experimental net photosynthesis rate is not significantly different among the different gravity levels (Figure 9), 9% higher at 1g and 2g than at 0g, whereas at high light settings (500 $\mu mol\, m^{-2}\, s^{-1}$) it is 36 to 63% higher at 1g and 2g than at 0g. This can be explained by the fact that at low light, photosynthesis is limited by incoming light and thus the magnitude of changes resulting from lower gravity levels is much lower. This effect is less visible on simulation results, where net photosynthesis rate is respectively at low and high light, 26% and 34% greater at 1g than at 0g, and 30% and 39 % greater at 2g than at 0g. This discrepancy in the results could be explained by the fact that the model does not include the respiration rate and so the simulation results are actually a gross photosynthesis rate and not the net photosynthesis rate as reported by Kitaya et al. [45].

Consequently, there are threshold values for gravity, ventilation, light, and stomatal conductance for water vapor, which dictate the magnitude of changes in leaf surface temperature and photosynthesis rate. Light levels and values of stomatal conductance for water vapor determine the maximum gas exchange rates; they are limited by ventilation under a certain threshold value; and they are further limited under a certain gravity threshold level.

4.2. Sensitivity to leaf shape

The effect of leaf shape on leaf surface temperature for a given surface area is the most significant for the highest ventilation (1 m/s) because this is the case where gas exchange is the largest, hence the magnitude of changes due to leaf shapes are largest too. Similarly the difference in leaf surface temperature between a rectangular-shaped and a circular-shaped leaf is not significant at 0g and low ventilation.

The study here was made on a 2-cm wide leaf because the width of the barley leaf used in the experiments reported by Kitaya et al. was approximately 2 cm. This resulted in a larger characteristic length for the rectangular-shaped leaf

than for the circular-shaped one. The sensitivity to different leaf shapes could be further studied with equal characteristic length and equal surface area, for a more thorough analysis of leaf shape influence on leaf surface temperature.

4.3. Model use

Practically, since this model fits experimental data on dynamic response, it could be used to identify needed parameters like stomatal conductance for water vapor with short-time experiments. The steps to use this model for plant growth and gas exchange predictions in reduced gravity environments would be as follows:

- define environmental plant growth conditions along with the species and cultivar to be grown;
- grow plants of interest in these environmental conditions in 1g;
- perform leaf surface temperature and net photosynthesis measurements;
- use the model to identify the stomatal conductance for water vapor in different ventilation and light settings;
- use the model with these values of stomatal conductance for water vapor to predict plant growth in different gravity environments.

4.4. Concluding remarks

4.4.1. Validation in non-standard conditions

The fact that the model presented here can fit experimental data obtained in a plane (i.e. reduced total pressure and low relative humidity), with different lighting and ventilation settings, as well as different initial leaf surface temperature, shows its robustness for a wide range of environmental parameters. The sensitivity study to a large spectrum of leaf absorbance and stomatal conductance for water vapor, in three widely spread ventilation settings, also shows that this model is broadly applicable.

4.4.2. Potentialities of the model

Despite ample evidence of impaired photosynthesis rates and gas exchange in microgravity environments [20, 45, 50, 51], little effort has been made to model these variables in low gravity and predict their behavior in non-terrestrial conditions. The results presented here show strong evidence that a mechanistic modeling approach to gas exchange and plant growth in reduced gravity environments will enable a better understanding of the intricate relationships between the different parameters involved but also enable us to identify adequate conditions for plant growth in space.

This emphasizes the main difference between our approach compared to previous work on plant growth and gas exchange modeling: for life-support systems, we need to use mechanistic models to deeply understand mechanisms involved in physical, chemical, and biological processes and to later predict how much biomass can be harvested, how much CO_2 can be scrubbed and how much O_2 can be produced, and how much water can be recycled. Typical models addressing plants' leaf surface temperatures in 1g, energy balances, and gas exchange use experimental measurements of these parameters to deduce stomatal conductance for water vapor [18] or make use of semi-empirical parameters with Farquhar et al. [41] photosynthesis model [17, 49] or Jarvis stomatal model [39].

The focus here was set on leaf surface temperature, which is a good indicator of transpiration rate and water status in the leaf, as detailed in equation 52, and directly related to gas exchange at the leaf surface. However, as shown in part 3.2.2, this mechanistic model can also predict with a good accuracy the order of magnitude of the photosynthesis rate in various gravity and light levels. To increase the precision of this prediction, the respiration rate should be included into the model; it was not the focus here, since the scope of this study was the short-term physical response of the leaf's photosynthetic activity and dynamic behaviour. Nevertheless, this paves the way for longer term response predictions, such as the biological and growth responses of a leaf, linked to steady-state behaviour and biomass production. Eventually, these types of

mechanistic models could allow the computation of carbon dioxide uptake rate and water transpiration rate in reduced gravity conditions, such as weightlessness, Lunar or Martian conditions.

Acknowledgements

The authors would like to acknowledge the Centre National de la Recherche Scientifique (CNRS) and the Centre National d'Etudes Spatiales (CNES) who funded this work as part of a three-year PhD fellowship. We would like to express our gratitude to the anonymous reviewers who helped us make this manuscript more intelligible to a wider audience. We also deeply thank Michael Gildersleeve for proofreading the manuscript, and Dr. Gioia Massa and Dr. Ray Wheeler for insightful comments and discussions over this study.

References

[1] C. Lasseur, J. Brunet, M. De Weever, H.and Dixon, C.-G. Dussap, F. Godia, N. Leys, M. Mergeay, D. Van Der Straeten, Melissa: The european project of closed life support system, Gravitational and Space Biology 23 (2) (2010) 3 – 12.

[2] M. S. Anderson, M. K. Ewert, J. F. Keener, Life support baseline values and assumptions document, Tech. rep., NASA (January 2018).

[3] L. Poughon, C.-G. Dussap, J.-B. Gros, Preliminary study and simulation of the melissa loop including a higher plants compartment, in: Sixth European Symposium on Space Environmental Control Systems, T.-D. Guyenne. European Space Agency, 1997, p. 879.

[4] J. Gros, L. Poughon, C. Lasseur, A. Tikhomirov, Recycling efficiencies of c,h,o,n,s, and p elements in a biological life support system based on microorganisms and higher plants, Advances in Space Research 31 (1) (2003) 195 – 199. doi:https://doi.org/10.1016/S0273-1177(02)00739-1.

[5] R. M. Wheeler, Carbon balance in bioregenerative life support systems: Some effects of system closure, waste management, and crop harvest index, Advances in Space Research 31 (1) (2003) 169 – 175. doi:https://doi.org/10.1016/S0273-1177(02)00742-1.

[6] R. M. Wheeler, Plants for human life support in space: From myers to mars, Gravitational and Space Biology 23 (2) (2010) 26 – 36.

[7] R. M. Wheeler, Agriculture for space: People and places paving the way, Open Agriculture 2 (1) (2017) 14–32. doi:https://doi.org/10.1515/opag-2017-0002.

[8] P. Hézard, Higher Plant Growth Modelling for Life Support Systems: Global Model Design and Simulation of Mass and Energy Transfers at the Plant Level., PhD thesis, Doctoral school of Life Sciences, Health,

Agronomy, Environment. Université Blaise Pascal, Université d'Auvergne, Clermont-Ferrand (2012).

[9] L. Poulet, J.-P. Fontaine, C.-G. Dussap, Plant's response to space environment: a comprehensive review including mechanistic modelling for future space gardeners, Botany Letters 163 (3) (2016) 337–347. doi:10.1080/23818107.2016.1194228.

[10] B. Farges, L. Poughon, C. Creuly, J.-F. Cornet, C.-G. Dussap, C. Lasseur, Dynamic aspects and controllability of the melissa project: A bioregenerative system to provide life support in space, Applied Biochemistry and Biotechnology 151 (2) (2008) 686. doi:10.1007/s12010-008-8292-2.

[11] J. H. M. Thornley, I. R. Johnson, Plant and crop modelling: a mathematical approach to plant and crop physiology, Clarendon Press, 1990.

[12] P. Hézard, S. Sasidharan, C. Creuly, C.-G. Dussap, Higher plants modeling for bioregenerative life support applications: general structure of modeling, in: 40th International Conference on Environmental Systems, International Conference on Environmental Systems (ICES), American Institute of Aeronautics and Astronautics, 2010. doi:10.2514/6.2010-6079.

[13] G. Lopez, R. R. Favreau, C. Smith, T. M. DeJong, L-PEACH: A Computer-based Model to Understand How Peach Trees Grow, HortTechnology 20 (6) (2010) 983–990. doi:https://doi.org/10.21273/HORTSCI.20.6.983.

[14] L. Ordoñez, C. Lasseur, L. Poughon, G. Waters, MELiSSA Higher Plants Compartment Modeling using EcosimPro, SAE Technical Paper (2004-01-2351). doi:10.4271/2004-01-2351.

[15] A. McCormack, B. Bugbee, O. Monje, R. Sirko, A method for modeling transpiration in celss, in: AlAA Space Programs and Technobgies Conference, American Institute of Aeronautics and Astronautics, 1994. doi:10.2514/6.1994-4573.

[16] T. Volk, B. Bugbee, R. M. Wheeler, An approach to crop modeling with the energy cascade., Life support and biosphere science : international journal of earth space 1 (3-4) (1995) 119–127.

[17] S. J. Schymanski, D. Or, M. Zwieniecki, Stomatal Control and Leaf Thermal and Hydraulic Capacitances under Rapid Environmental Fluctuations, PLOS One 8 (1) (2013) e54231. doi:10.1371/journal.pone.0054231.

[18] S. Vialet-Chabrand, T. Lawson, Dynamic leaf energy balance: deriving stomatal conductance from thermal imaging in a dynamic environment, Journal of Experimental Botany 70 (10) (2019) 2839–2855. doi:10.1093/jxb/erz068.

[19] S. B. J. A. Farquhar, G. D.and Von Caemmerer, A biochemical model of photosynthetic co2 assimilation in leaves of c3 species, Planta 149 (1980) 78–90. doi:https://doi.org/10.1007/BF00386231.

[20] Y. Kitaya, M. Kawai, J. Tsuruyama, H. Takahashi, A. Tani, E. Goto, T. Saito, M. Kiyota, The effect of gravity on surface temperatures of plant leaves, Plant, Cell & Environment 26 (4) (2003) 497–503. doi:10.1046/j.1365-3040.2003.00980.x.

[21] O. Monje, G. Stutte, D. Chapman, Microgravity does not alter plant stand gas exchange of wheat at moderate light levels and saturating CO2 concentration, Planta 222 (2) (2005) 336–345. doi:10.1007/s00425-005-1529-1.

[22] M. Yamashita, Y. Ishikawa, Y. Kitaya, E. Goto, M. Arai, H. Hashimoto, K. Tomita-Yokotani, M. Hirafuji, K. Omori, A. Shiraishi, A. Tani, K. Toki, H. Yokota, O. Fujita, An overview of challenges in modeling heat and mass transfer for living on mars, Annals of the New York Academy of Sciences 1077 (2006) 232—243. doi:10.1196/annals.1362.012.

[23] C.-G. Dussap, Concept of the control system architecture of the MELiSSA loop, Barcelona, 2018.

[24] A. Kichah, P.-E. Bournet, C. Migeon, T. Boulard, Measurement and CFD simulation of microclimate characteristics and transpiration of an Impatiens pot plant crop in a greenhouse, Biosystems Engineering 112 (1) (2012) 22–34. doi:10.1016/j.biosystemseng.2012.01.012.

[25] P. H. Schuepp, Tansley Review No. 59 Leaf boundary layers, New Phytologist 125 (3) (1993) 477–507. doi:10.1111/j.1469-8137.1993.tb03898.x.

[26] J. J. Landsberg, A. S. Thom, Aerodynamic properties of a plant of complex structure, Quarterly Journal of the Royal Meteorological Society 97 (414) (1971) 565–570. doi:10.1002/qj.49709741418.

[27] A. S. Thom, Momentum, mass and heat exchange of vegetation, Quarterly Journal of the Royal Meteorological Society 98 (415) (1972) 124–134. doi:10.1002/qj.49709841510.

[28] S. Sasidharan, P. Hezard, L. Poughon, C.-G. Dussap, Higher Plant Modelling For Bio-regenerative Life Support Including Metabolic Pathways Description, in: 40th International Conference on Environmental Systems, American Institute of Aeronautics and Astronautics, 2010. doi:10.2514/6.2010-6192.

[29] W. J. Beek, K. M. K. Muttzall, J. W. v. Heuven, Transport phenomena, 2nd Edition, Chichester ; New York : Wiley, 1999.

[30] R. Bird, W. Stewart, E. Lightfoot, Transport phenomena, 2nd ed., John Wiley Editor, 2002.

[31] H. Lambers, F. S. Chapin, T. L. Pons, Plant Physiological Ecology, 2nd Edition, Springer, 2008.

[32] A. Tuzet, A. Perrier, R. Leuning, A coupled model of stomatal conductance, photosynthesis and transpiration, Plant, Cell & Environment 26 (7) (2003) 1097–1116. doi:10.1046/j.1365-3040.2003.01035.x.

[33] T. K. Sherwood, R. Pigford, C. Wilke, Mass Transfer, McGraw-Hill Inc.,US, New York, 1975.

[34] P. V. Danckwerts, Gas-liquid reactions, new york Edition, Chemical Engineering Series, McGraw-Hill Book Co., 1970.

[35] H. Schlichting, K. Gersten, Fundamentals of boundary layer theory, in: Boundary-Layer Theory, Springer, Berlin, Heidelberg, 2017, pp. 29–49.

[36] R. M. Wheeler, C. L. Mackowiak, N. C. Yorio, J. C. Sager, Effects of CO2 on Stomatal Conductance: Do Stomata Open at Very High CO2 Concentrations? , Annals of Botany 83 (3) (1999) 243–251. doi:10.1006/anbo.1998.0813.

[37] G. Damour, T. Simonneau, H. Cochard, L. Urban, An overview of models of stomatal conductance at the leaf level, Plant, Cell & Environment 33 (9) (2010) 1419–1438. doi:10.1111/j.1365-3040.2010.02181.x.

[38] T. N. Buckley, K. A. Mott, Modelling stomatal conductance in response to environmental factors, Plant, Cell & Environment 36 (9) (2013) 1691–1699. doi:10.1111/pce.12140.

[39] J. Ngao, B. Adam, M. Saudreau, Intra-crown spatial variability of leaf temperature and stomatal conductance enhanced by drought in apple tree as assessed by the ratp model, Agricultural and Forest Meteorology 237-238 (2017) 340 – 354. doi:https://doi.org/10.1016/j.agrformet.2017.02.036.

[40] Q. Gao, P. Zhao, X. Zeng, X. Cai, W. Shen, A model of stomatal conductance to quantify the relationship between leaf transpiration, microclimate and soil water stress, Plant, Cell & Environment 25 (11) (2002) 1373–1381. doi:10.1046/j.1365-3040.2002.00926.x.

[41] G. D. Farquhar, T. D. Sharkey, Stomatal conductance and photosynthesis, Annual Review of Plant Physiology 33 (1) (1982) 317–345. doi:10.1146/annurev.pp.33.060182.001533.

[42] O. C. Bridgeman, E. W. Aldrich, Vapor Pressure Tables for Water, Journal of Heat Transfer 86 (2) (1964) 279–286. doi:10.1115/1.3687121.

[43] National Institute of Standards and Technology, Water, in: NIST Chemistry WebBook NIST Standard Reference Database Number 69, U.S. Secretary of Commerce, 2017.

[44] L. Poulet, J.-P. Fontaine, C.-G. Dussap, A physical modeling approach for higher plant growth in reduced gravity environments, Astrobiology 18 (9) (2018) 1093–1100, pMID: 30067083. doi:10.1089/ast.2017.1804.

[45] Y. Kitaya, M. Kawai, H. Takahashi, A. Tani, E. Goto, T. Saito, M. Shibuya, T Kiyota, Heat and gas exchanges between plants and atmosphere under microgravity conditions, Annals of the New York Academy of Sciences 1077 (2006) 244–255. doi:10.1196/annals.1362.027.

[46] J. A. Nelson, B. Bugbee, Analysis of environmental effects on leaf temperature under sunlight, high pressure sodium and light emitting diodes, PLOS One 10 (10). doi:10.1371/journal.pone.0138930.

[47] C. A. Mitchell, Bioregenerative life-support systems, The American Journal of Clinical Nutrition 60 (5) (1994) 820S–824S. doi:10.1093/ajcn/60.5.820S.

[48] C. A. Mitchell, Influence of mechanical stress on auxin-stimulated growth of excised pea stem sections, Physiologia Plantarum 41 (2) (1977) 129–134. doi:10.1111/j.1399-3054.1977.tb05543.x.

[49] S. J. Schymanski, D. Or, Wind increases leaf water use efficiency, Plant, Cell & Environment 39 (7) (2016) 1448–1459. doi:10.1111/pce.12700.

[50] Y. Kitaya, M. Kawai, J. Tsuruyama, H. Takahashi, A. Tani, E. Goto, T. Saito, M. Kiyota, The effect of gravity on surface temperature and net photosynthetic rate of plant leaves, Advances in Space Research 28 (4) (2001) 659–664. doi:10.1016/S0273-1177(01)00375-1.

[51] O. Monje, G. Bingham, J. Carman, W. Campbell, F. Salisbury, B. Eames, V. Sytchev, M. Levinskikh, I. Podolsky, Canopy photosynthesis and transpiration in micro-gravity: Gas exchange measurements aboard mir, Advances in Space Research 26 (2) (2000) 303 – 306, life Sciences: Space Life Support Systems and the Lunar Farside Crater SAHA Proposal. doi:https://doi.org/10.1016/S0273-1177(99)00575-X.